

MathScape: Evaluating MLLMs in multimodal Math Scenarios through a Hierarchical Benchmark

Minxuan Zhou^{1*}, Hao Liang^{2*}, Tianpeng Li³, Zhiyu Wu³, Mingan Lin³, Linzhuang Sun⁴, Yaqi Zhou³, Yan Zhang³, Xiaoqin Huang³, Yicong Chen³, Yujing Qiao³, Weipeng Chen³, Bin Cui², Wentao Zhang^{2†}, Zenan Zhou^{3†}

¹Nankai University ²Peking University ³Baichuan Inc. ⁴University of Chinese Academy of Sciences
zhouminxuan@mail.nankai.edu.cn, hao.liang@stu.pku.edu.cn, wentao.zhang@pku.edu.cn, zhouzenan@baichuan-inc.com

Abstract

With the development of Multimodal Large Language Models (MLLMs), the evaluation of multimodal models in the context of mathematical problems has become a valuable research field. Multimodal visual-textual mathematical reasoning serves as a critical indicator for evaluating the comprehension and complex multi-step quantitative reasoning abilities of MLLMs. However, previous multimodal math benchmarks have not sufficiently integrated visual and textual information. To address this gap, we proposed MathScape, a new benchmark that emphasizes the understanding and application of combined visual and textual information. MathScape is designed to evaluate photo-based math problem scenarios, assessing the theoretical understanding and application ability of MLLMs through a categorical hierarchical approach. We conduct a multi-dimensional evaluation on 11 advanced MLLMs, revealing that our benchmark is challenging even for the most sophisticated models. By analyzing the evaluation results, we identify the limitations of MLLMs, offering valuable insights for enhancing model performance. The code is made available <https://github.com/PKU-Baichuan-MLSystemLab/MathScape>.

1 Introduction

In recent years, there have been advancements in large language models (LLMs) (OpenAI 2023a; Touvron et al. 2023) and MLLMs (Zhao et al. 2023; Wu et al. 2023; Bai et al. 2024). They have shown strong understanding ability among different modalities (Liu et al. 2023b; Bai et al. 2023b).

Among Multimodal Large Language Models (MLLMs), Vision Language Large Models (VLLMs) have demonstrated competitive performance in traditional multimodal tasks, including image classification (Chen et al. 2024), image understanding (Li et al. 2023b,c), and image captioning (Bai et al. 2023b). Furthermore, their advanced language understanding capabilities contribute to strong performance in text-rich tasks, such as visual question answering (Liu et al. 2023b,a) and image-text retrieval (Chen et al. 2024). Recently, VLLMs have also shown significant

progress in solving mathematical problems. Therefore, comprehensive benchmarks are essential to evaluate the mathematical abilities of VLLMs. Although several benchmarks, such as MATH-V (Wang et al. 2024a), MathVerse (Zhang et al. 2024), and MathVista (Lu et al. 2023b), have been developed to assess the mathematical capabilities of VLLMs. They primarily focus on a combination of text math problems and image figures. Also, they only use simple metrics and lack effective evaluation for complex or extended responses. Consequently, they face two key challenges:

C1. Insufficient Real-World Data. In previous datasets like MATH-V (Wang et al. 2024a), MathVerse (Zhang et al. 2024), and MathVista (Lu et al. 2023b), the mathematical description was typically provided as text input, while the image contained only figures. This approach doesn't align well with real-world scenarios, where both the mathematical description and figures are captured together in a single image.

C2. Absence of Effective Evaluation Metrics. In previous datasets (Wang et al. 2024a; Zhang et al. 2024; Lu et al. 2023b), the evaluation was limited to short answers, lacking the ability to assess long-form responses.

To address these issues, we implement a three-step pipeline for constructing a real-world math image dataset. As illustrated in Figure 3, the process begins by converting math documents into images, as shown in Figure 2. Next, we capture photos and screenshots to build the dataset. Finally, we perform a thorough review and knowledge classification to ensure the dataset's high quality. For evaluation, we design a two-step pipeline specifically for assessing longer math problems. First, we use LLMs to extract answers for each subproblem. Then, we employ LLMs as evaluators to assess the correctness of each solution. With the data construction and evaluation pipeline, we constructed MathScape, a new multimodal dataset that combines photos of real-world math problems with their correct answers.

The core contributions are summarized as follows:

- **New Perspective:** To the best of our knowledge, we are the first to construct images that combine both figures and mathematical text descriptions, closely mirroring real-world scenarios.
- **New Method:** We propose a novel three-step dataset

*These authors contributed equally.

†Corresponding author.

Copyright © 2025, Association for the Advancement of Artificial Intelligence (www.aaai.org). All rights reserved.

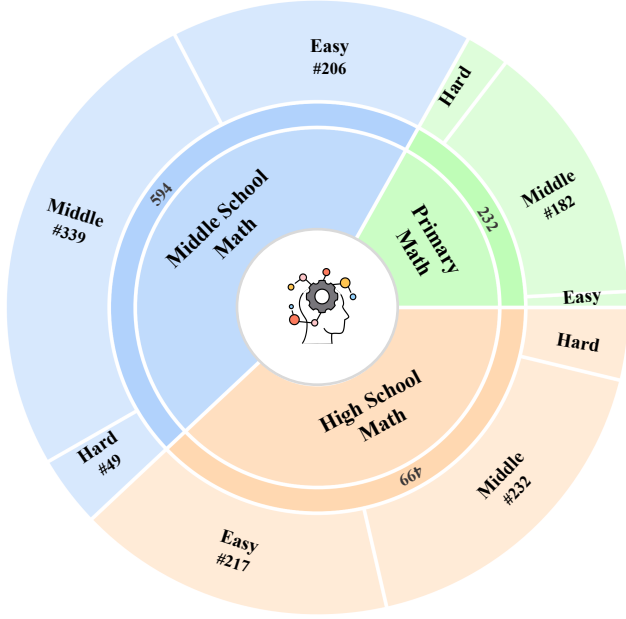


Figure 1: MathScape offers a comprehensive collection of math problems from primary school to high school. The problems range in difficulty from easy to difficult, catering to various levels of evaluation.

construction pipeline, as illustrated in Figure 3. Additionally, we introduce a new two-step evaluation method specifically designed for assessing long answers.

- **New Benchmark:** We present MathScape, a new multimodal mathematical dataset that spans various difficulty levels, question types, and knowledge areas, providing a comprehensive tool to evaluate the mathematical capabilities of MLLMs. Moreover, MathScape is entirely original, consisting of previously unreleased multimodal mathematical data.

2 Related Work

In the field of MLLMs, the benchmark for multimodal mathematical reasoning capability represents a significant and novel research direction. Mathematical reasoning is a crucial indicator for evaluating the ability of LLMs to perform complex, multi-step reasoning and quantitative analysis within visual contexts. Below, we highlight some relevant work and the latest developments in this area.

2.1 Benchmark for Mathematical Evaluation

Recent research has seen significant advancements in mathematical reasoning benchmarks aimed at evaluating mathematical abilities. In this summary, we review both pure text and multimodal math benchmarks.

Pure Text Benchmarks GSM8K (Cobbe et al. 2021) is a dataset from OpenAI that includes 8.5K high-quality elementary school math word problems, each requiring 2 to 8 steps to solve. These problems primarily involve basic

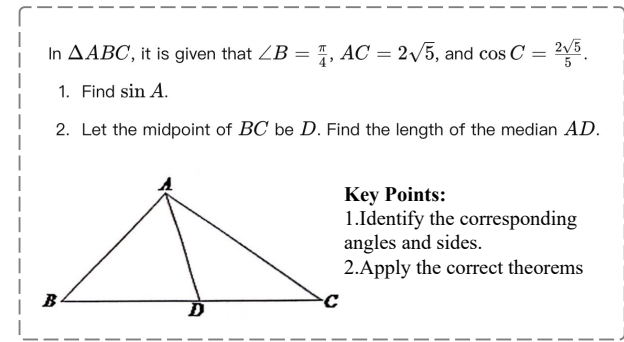


Figure 2: An problem example of MathScape. Examples in MathScape are represented by images taken by humans, ensuring a more realistic scenario. Each example will contain a correct answer.

arithmetic operations such as addition, subtraction, multiplication, and division. MATH (Hendrycks et al. 2021) offers a dataset of 12,500 problems sourced from high school math competitions. SuperCLUE-Math (Xu et al. 2024a) is a Chinese benchmark for multi-step reasoning in mathematics, containing over 2,000 problems that require multi-step reasoning and offer natural language solutions. MathBench (Liu et al. 2024b) includes 3,709 math problems ranging from basic arithmetic to college-level questions, covering multiple difficulty levels.

All these benchmarks focus exclusively on text-based mathematical tasks. They are designed to evaluate the mathematical capabilities of LLMs through specialized problem sets.

Multimodal Benchmarks With the rapid advancement of MLLMs, several high-quality benchmarks have emerged to evaluate mathematical problem-solving in visual contexts. MathVista (Lu et al. 2023b) focuses on visual math QA tasks, assessing model performance across various math domains, such as arithmetic and algebra, using visual scenarios. MATH-V (Wang et al. 2024a) is another benchmark that targets multimodal mathematical understanding, with questions primarily sourced from math competitions. MathVerse (Zhang et al. 2024) evaluates MLLMs' comprehension of visual diagrams using CoT (Chain of Thought) strategies on 2,612 multimodal math problems. CMMU (He et al. 2024) is a large-scale Chinese benchmark for multi-disciplinary, multimodal understanding, featuring questions from college exams and textbooks.

Compared to these existing multimodal mathematical benchmarks, which often have limitations in question length, complexity, and openness to model answers, our MathScape benchmark is designed to be longer and more open-ended.

2.2 MLLMs for Mathematics

Commonly Used VLLMs The integration of visual knowledge into LLMs has become a pivotal area of research due to the rapid advancements in LLMs. VLLMs combine vision information from vision encoders with LLMs, thus enabling these models to process and interpret visual inputs

for various visual tasks (Liu et al. 2023c; Zhang et al. 2022; Li et al. 2022b) with enhanced accuracy and efficiency. Pioneering frameworks like CLIP (Radford et al. 2021) leverage contrastive learning on expansive image-caption datasets to align modalities, forming the groundwork for cross-modal comprehension. Various adapters (Liu et al. 2023b,a; Li et al. 2023b, 2022a; Jian, Gao, and Vosoughi 2023; Lu et al. 2023a) are introduced to further integrate different modalities. For example, LLaVA (Liu et al. 2023b,a) employs a straightforward MLP to inject the vision information into LLMs. Whereas more complex implementations like the Q-Former in BLIP (Li et al. 2022a, 2023b) utilize cross-attention to enhance modality integration.

Recent studies (Wang et al. 2024b; Chen et al. 2023; Liu et al. 2023b,a; Li et al. 2023a) aims to boost VLLM performance by focusing on the quality of both pre-training and fine-tuning datasets. Models like LLaVA (Liu et al. 2023b,a) and ShareGPT4V (Chen et al. 2023) have shown remarkable advancements in understanding and following complex instructions through instruction tuning.

VLLMs Designed for Math Problems MAMmoTH (Yue et al. 2023) InternLM-Math (Ying et al. 2024), and ChatGLM-Math (Xu et al. 2024b) are multimodal models specifically tailored for dealing with mathematical questions, incorporating both textual and visual components in their problem design to enhance their ability to handle complex mathematical tasks.

3 Methodology

We begin by introducing the construction pipeline of MathScape in Section 3.1. Next, we present the multidimensional evaluation approach in Section 3.2. In Section 3.3, we detail the two-step answer evaluation method. Finally, we summarize the dataset statistics in Section 3.4.

3.1 Construction of MathScape

Data Preparation The data preparation module consists of three steps, as shown in Figure 3(a). First, we collected a large number of mathematics questions from elementary, junior high, and senior high school exams and homework as the evaluation sample. We gathered a total of 1,325 image mathematics questions. Next, the question documents were converted to PDF format using Pandoc and subsequently transformed into images for further use.

Data Annotation As illustrated in Figure 3(b), the images are then transformed to closely align with real-world scenarios by capturing photos of printed images, screen displays, and using screenshots.

Data Check and Knowledge Classification After constructing the dataset, we perform a double-check and knowledge-based classification to ensure its high quality. As illustrated in Figure 3(c), we rigorously review the dataset to ensure that both the textual and graphical inputs are clear and accurate. Once data quality is verified, we categorize the data according to knowledge points.

3.2 Multidimensional Evaluation

To comprehensively evaluate the performance of VLLMs, we designed multiple dimensions to classify and assess their mathematical abilities across various categories. The classification types we used are as follows:

Question Types: We first categorized the test questions into different types, such as multiple-choice, fill-in-the-blank (Solution), and proof questions, to examine the model’s performance across various question formats.

Knowledge Points: We also classified the questions based on mathematical knowledge areas, including algebra, geometry, probability, and statistics, to assess the model’s proficiency in different domains of mathematics.

Educational Stages: Additionally, the questions were divided according to the educational stage—primary school, middle school, and high school—to evaluate the model’s adaptability and accuracy at different levels of education.

3.3 Evaluation Method

We utilize a two-step evaluation process to effectively score long answers.

Answer Segmentation: As illustrated in Figure 4, we prompt the LLMs to decompose a lengthy answer into multiple sub-answers, each one focusing on a specific aspect of the problem. This segmentation ensures that the complex answer is broken down into manageable components, making it easier to evaluate the correctness and relevance of each part. By isolating sub-problems within the overall solution, we can achieve a more granular analysis of the model’s performance.

Sub-Answer Scoring: After segmenting the long answer, we employ the prompt depicted in Figure 12 to automatically score each sub-answer individually. This method allows us to evaluate the accuracy of each component independently, ensuring that the final score reflects the model’s ability to handle various aspects of the problem comprehensively. By scoring sub-answers separately, we can identify specific areas where the model excels or struggles, providing deeper insights into its strengths and weaknesses.

3.4 Dataset Statistics

In this section, we provide a summary of the statistics for our MathScape dataset. The dataset primarily consists of Chinese image-text problems, along with question labels, attribute information, problem-solving processes, and standard reference answers. Detailed statistics are presented in Figure 5.

As shown in Figure 5(a), our dataset thoughtfully incorporates the characteristics of multimodal image-text questions. A significant portion of the questions are geometric, which often require the integration of images for effective problem-solving. In contrast, topics like equations and inequalities are less represented, aligning more closely with the specific demands of multimodal assessment.

Figure 5(b) illustrates that our dataset primarily includes solution questions and multiple-choice questions, with fewer

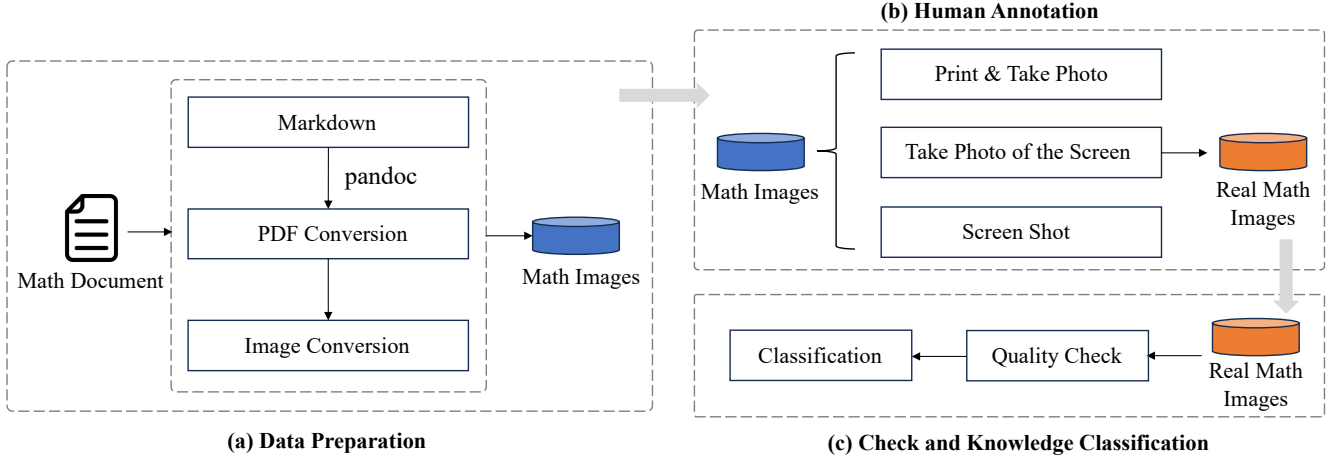


Figure 3: MathScape process pipeline.

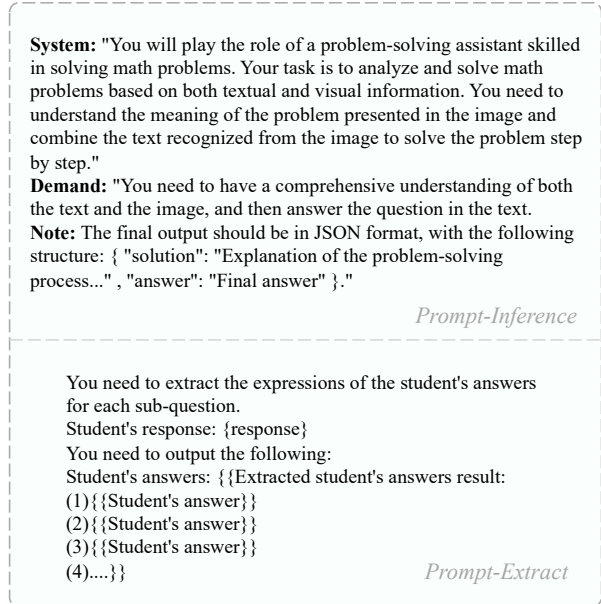


Figure 4: Prompts for inference and extracting answers.

proof questions. This distribution indicates that our dataset is designed to challenge models with diverse question types, while still reflecting the real-world emphasis on practical problem-solving.

Overall, our dataset contains a total of 1,325 images, providing a robust resource for evaluating the mathematical reasoning capabilities of MLLMs.

4 Experiments and Analysis

In this section, we utilize multiple state-of-the-art (SOTA) models and test their performance on the MathScape benchmark.

4.1 Experimental Setups

Models. In our evaluation of multimodal LLMs, we focused on both open-source and closed-source models that

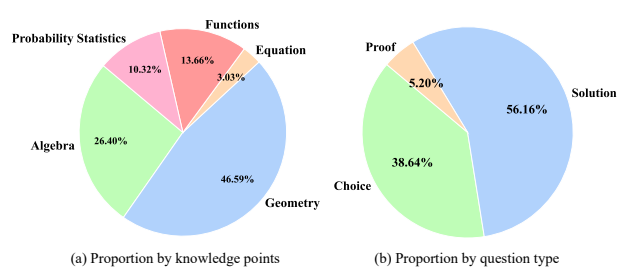


Figure 5: Proportion Figure

rank among the top performers on major multimodal LLM leaderboards. This included 11 different types of VLLMs, with a particular emphasis on analyzing the results and performance of the leading models.

- Closed-source models: GPT4 (OpenAI 2023b), GeminiPro (Reid et al. 2024), Claude-3-Opus, Baichuan-VL (Yang et al. 2023), Qwen-Max (Bai et al. 2023a), Qwen-Plus (Bai et al. 2023a), GLM4V.
- Open-source models: Deepseek-VL(Lu et al. 2024), LLaVA(Liu et al. 2024a), Yi(Young et al. 2024).

Settings. We conduct all model inferences in a zero-shot setting, using the same configuration for each official model. Instead of the Chain of Thought (CoT) technique, we use a custom prompt to guide the model in producing the problem-solving process and final answer, as shown in Figure 4. The settings include a max token limit of 2048, top-k of 5, a temperature of 0.3, and a repetition penalty of 1.05. All experiments are run on NVIDIA H100 GPUs.

4.2 Performance of Various Models

In this section, we present the performance of commonly used MLLMs on our benchmark. We analyze the results from the perspectives of Question Types, Knowledge Points, and Educational Stages:

Question Types As shown in Table 1, GPT-4V and GPT-4-turbo exhibits the highest accuracy across all question

Table 1: Accuracy scores comparison of models on different question types

Model	Average	Choice	Solution	Proof
Closed-source Models				
GPT-4V	34.96	35.75	31.72	28.33
GPT-4-turbo	33.92	29.85	31.58	56.62
Claude-3-Opus	28.79	29.3	20.85	50.00
Gemini-Pro	21.37	12.62	16.16	37.50
Baichuan-VL	30.00	26.38	25.83	45.97
Qwen-VL-Max	27.83	23.97	22.17	34.85
Qwen-VL-Plus	15.60	19.46	12.48	35.19
GLM4V	12.26	11.54	7.31	26.28
Open-source Models				
Yi-VL-34B	18.36	19.01	9.98	33.33
DeepSeek-V2	15.66	12.75	10.60	37.69
LLaVA-1.6-7B	12.35	11.31	6.24	13.43

types, with an average of 34.96%, followed by GPT-4-Turbo Vision at 33.92%. While Yi-VL-34B and DeepSeek-V2 achieve good performance among open-source models. We can see the performance of closed-source models achieved better performance than open-source models.

The table shows that models generally perform better on proof questions compared to multiple-choice and solution questions. This suggests that the structured format and clear information in proof questions make them easier for models to handle, while solution questions, which require complex, multi-step reasoning, pose more of a challenge.

Knowledge Points Table 2 shows the answer accuracy of the models in different knowledge points. GPT-4V and GPT-4-turbo consistently outperform other models in areas like algebra, equations and inequalities, functions, and probability and statistics. Most models show balanced performance across different knowledge areas, but there are exceptions, such as LLaVA-1.6, which does well in equations and inequalities but struggles with functions.

Overall, closed-source models are more accurate than open-source ones, with GPT-4V and GPT-4-turbo leading in many categories.

Educational Stages Table 3 presents the performance of open-source and closed-source models on MathScape at the elementary, middle, and high school levels. At the elementary and middle levels, the models perform similarly. However, when the difficulty increases to the high school level, we observe a significant drop in accuracy. Some models show an extreme decrease in performance between the middle and high school benchmarks. For instance, Gemini-Pro has an average accuracy of 25.79% at the elementary level, but this sharply declines to just 10.22% at the high school level. This suggests that high school-level math poses significant challenges for LLMs.

Overall, our evaluation shows that closed-source models, particularly GPT-4V and GPT-4-turbo, consistently outperform open-source models across various question types,

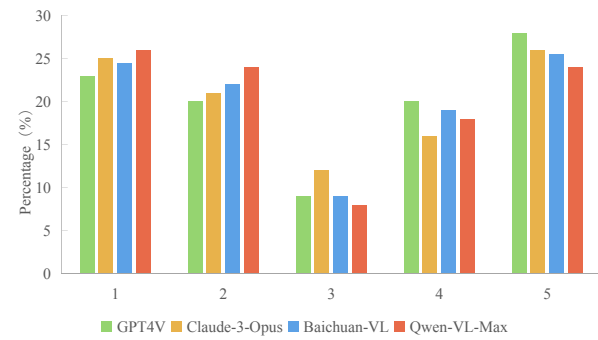


Figure 6: Stability Analysis: For each problem, the model is tested five times. The numbers 1 to 5 represent the proportion of correct responses.

knowledge points, and educational stages. These models demonstrate superior accuracy, especially in structured question types like proof questions and in areas requiring advanced mathematical reasoning, such as algebra and probability. However, as the difficulty level increases, all models experience a decline in accuracy, with the most significant drops occurring between the middle and high school stages. GLM-4V performs particularly poorly at the high school level, highlighting the challenges that remain in achieving consistent performance on difficult math problems.

4.3 Stability Results and Analysis

In this subsection, we perform a stability test for GPT4V, Claude-3-Opus, Baichuan-VL, and Qwen-VL-Max. We selected 300 problems and tested each model five times on each problem. The number of correct answers across these attempts was calculated to assess the stability of each model. As shown in Figure 6, none of the models demonstrate high stability—only about 25% of the problems were answered correctly in all five attempts. Therefore, it's imperative to focus on enhancing the stability and robustness of math MLLMs, as consistent performance across repeated trials is crucial for their practical application in real-world scenarios. This finding also suggests that future research should explore methods to reduce variability in model outputs, ensuring more reliable and trustworthy results.

4.4 Answer Length and Accuracy

Distribution of Answer Lengths From Figure 7, we observe distinct patterns in the distribution of answer lengths across different models. Notably, GPT-4V and Baichuan-VL tend to generate a larger proportion of shorter answers. As illustrated in Figure 8, it is evident that shorter but accurate answers are more likely to achieve higher scores. This trend highlights the efficiency of models that can deliver concise and precise responses, particularly in scenarios where brevity is valued.

Analysis of Answer's Length In our evaluation of the MathScape benchmark, we observed that there is no straightforward positive correlation between answer length and accuracy. In fact, as shown in Figure 8, when the length of the answer increases, the accuracy tends to decrease.

Table 2: Accuracy scores comparison of Models on different knowledge points

Model	Algebraic	Geometric	Equations and Inequality	Functions	Probability Statistics
Closed-source Models					
GPT-4V	39.05	27.90	29.73	34.14	41.31
GPT4-turbo	36.28	29.54	32.50	28.43	37.99
Claude-3-Opus	31.78	22.67	20.83	20.58	36.22
Gemini-Pro	21.13	15.50	15.35	9.57	13.33
Baichuan-VL	30.54	25.98	25.83	26.69	23.67
Qwen-VL-Max	28.71	21.86	28.33	20.86	19.09
Qwen-VL-Plus	16.70	17.07	18.67	16.67	11.46
GLM4V	8.94	12.57	5.13	7.32	10.55
Open-source Models					
Yi-VL-34B	16.78	15.84	7.02	9.79	11.44
DeepSeek-V2	12.71	14.87	6.19	10.60	9.61
LLaVA-1.6-7B	9.76	8.58	15.79	3.57	10.77

Table 3: Comparison of Models on different knowledge stages (E: Easy, M: Medium, D: Difficult, Avg: Average Score)

Model	Elementary				Middle				High			
	avg	E	M	D	avg	E	M	D	avg	E	M	D
Closed-source Models												
GPT-4V	36.04	57.58	38.64	10.71	36.42	40.38	34.95	30.14	28.08	33.26	24.38	22.57
GPT4-turbo	37.71	72.73	38.79	18.33	35.12	37.22	34.51	30.44	26.06	28.65	25.19	18.83
Claude-3-Opus	28.30	33.33	31.10	10.04	31.04	31.29	33.97	12.22	19.17	24.07	16.41	15.15
Gemini-Pro	25.79	48.48	26.91	11.29	17.20	19.19	16.29	15.07	10.22	12.74	8.90	5.03
Baichuan-VL	29.85	35.00	31.45	18.33	29.96	28.94	32.57	21.38	22.33	27.59	17.42	16.01
Qwen-VL-Max	34.82	42.86	36.65	20.45	24.87	25.70	24.96	20.72	16.95	18.97	15.61	14.92
Qwen-VL-Plus	20.49	40.00	21.23	9.20	19.16	21.11	18.83	13.19	11.00	13.94	9.29	5.83
GLM4V	10.32	33.29	9.62	4.29	13.28	17.07	14.85	12.89	7.64	8.73	11.11	4.08
Open-source Models												
Yi-VL-34B	14.99	40.00	16.13	3.32	16.38	16.31	17.10	11.67	12.14	11.65	12.96	10.58
DeepSeek-V2	13.74	42.42	13.73	2.87	14.93	14.68	14.47	19.09	10.18	8.29	12.46	7.99
LLaVA-1.6-7B	9.77	35.21	10.82	7.12	10.37	9.79	10.90	9.07	7.57	8.41	6.53	4.54

This result demonstrates the robustness of the MathScape benchmark, ensuring that models cannot simply inflate their scores by producing longer answers. Such a design effectively prevents any biases in answering strategies, ensuring that the benchmark and evaluation method accurately reflects a model’s true ability to understand and solve mathematical problems, rather than gaining an unfair advantage through verbose responses.

5 Challenges and Future Directions

As shown in Section 4, none of the models performed well on our MathScape benchmark. In this section, we discuss the challenges faced by current MLLMs and suggest potential future directions for improving math MLLMs.

5.1 Challenges

In this subsection, we explore the main reasons why models provide incorrect answers to image-text mathematical

problems. These errors are mainly due to challenges in understanding and interpreting the information. We can break down these challenges into the following specific reasons:

Unable to Retrieve Information from the Image: This is one of the most common errors, where models may fail to extract all the relevant information from the image. For instance, when interpreting complex geometric patterns, it’s easy to overlook certain data or conditions, leading to incorrect answers. As shown in Case Study 1 in Figure 9, the model provided an incorrect proof due to its incomplete understanding of the image.

Misunderstanding of Graphic Positioning: This issue involves the accurate understanding of the spatial layout of graphics. For instance, in geometry problems, errors can occur if the model fails to correctly recognize the lengths or angles of figures. Such mistakes often stem from a lack of deep understanding of graphic properties or insufficient ability to shift perspectives. As illustrated in Figure 10, Case Study 2,

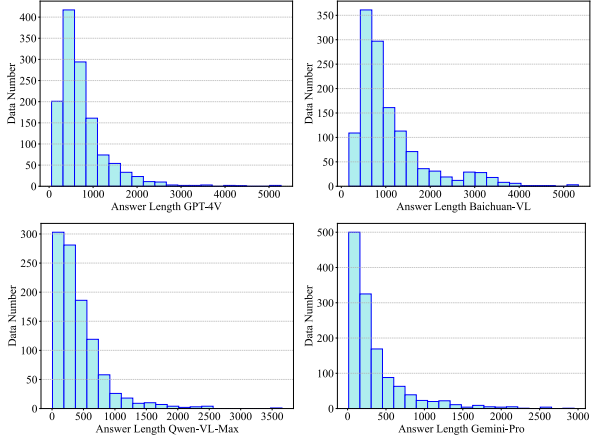


Figure 7: The variation of accuracy with answer length.

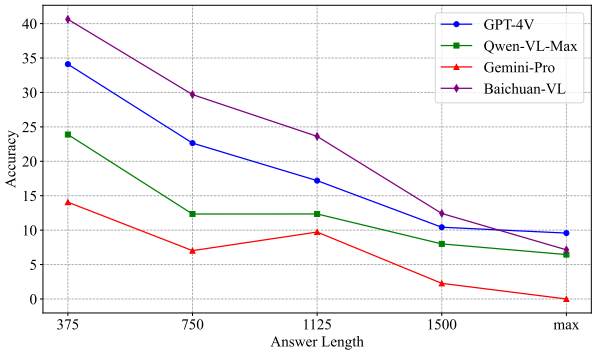


Figure 8: The variation of accuracy with answer length.

the model incorrectly interprets the distance from point A to 0 as $\sqrt{2}$.

Insufficient Reasoning Ability: This issue arises from the limited logical reasoning capabilities of LLMs. Even when the image information is provided correctly, the LLM may still produce incorrect responses. As shown in Case Study 3 in Figure 11, the LLM fails to solve the complex problem correctly and makes errors in the process.

Overall, the challenges for multimodal large models primarily focus on the interpretation of visual information and the inherent reasoning abilities of the models.

5.2 Future Directions for Math MLLMs

MathScape have introduced several challenges for MLLMs, as mentioned in section 5.1. In this section, we summarize future directions for MLLMs.

Stronger LLMs As discussed in section 5.1, it is evident that LLMs have limited mathematical reasoning abilities. To improve the math problem-solving capabilities of MLLMs, it is crucial to develop stronger LLMs with enhanced mathematical reasoning skills.

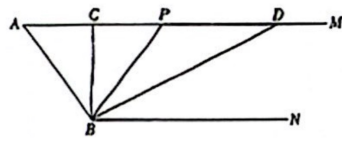
Better Pattern Recognition Improving pattern recognition is essential for enhancing the performance of MLLMs, particularly in tasks involving complex visual information.

Current models often struggle with identifying and interpreting intricate patterns in images, such as geometric configurations, charts, and fine-grained visual details. Future research should focus on developing models that can more accurately recognize and differentiate patterns, especially when they are complex.

6 Conclusion

Recently, MLLMs have emerged as powerful models for answering questions across multiple domains. However, comprehensive benchmarks that reflect real-world scenarios are needed to evaluate their mathematical performance. In this paper, we introduce MathScape, a new benchmark designed to assess the math capabilities of MLLMs using entirely original, leak-free images. Additionally, we propose a novel two-step evaluation method specifically for assessing long answers. MathScape not only challenges existing MLLMs but also aims to inspire the development of more advanced math-focused MLLMs.

Given the figure, it is known that $AM \parallel BN$, $\angle A=60^\circ$, point P is a moving point on the ray AM (not coincident with A), BC and BD bisect $\angle ABP$ and $\angle PBN$ respectively. The ray AM intersects C and D. (There needs to be a reasoning process, but it is not necessary to write out every step.)



1. Find the measure of $\angle CBD$
2. Prove that $\angle APB=2\angle ADB$
3. When point P moves such that $\angle ACB=\angle ABD$, find the measure of $\angle ABC$.

(a) Math Problem

First, since BD is the bisector of $\angle PBN$, similarly, we can conclude that $\angle PBD=\angle ABD=60^\circ$. Then, because $\angle APB=\angle ABP+\angle ABD$, we know that $\angle ABP=\angle ABC$ (since BC bisects $\angle ABP$), which equals 60° . Therefore, $\angle APB=60^\circ+60^\circ=120^\circ$. Now, we can calculate $\angle ADB$. Since $\angle ABD=60^\circ$, and we also know that $\angle BAD=60^\circ$, in the isosceles triangle ΔABD , $\angle ADB=180^\circ-\angle BAD-\angle ABD=180^\circ-60^\circ-60^\circ=60^\circ$. Therefore, we can say $\angle APB=120^\circ=2\times60^\circ=2\angle ADB$

(b) GPT4 Response

Judge: The proof is complete incorrect.
Difficulty: Recognition of spatial angle relationships, spatial deduction and proof.

(c) Challenges

Figure 9: Illustration of Case Study 1. The red sign marks the incorrect part of the answer.

References

Bai, J.; Bai, S.; Chu, Y.; Cui, Z.; Dang, K.; Deng, X.; Fan, Y.; Ge, W.; Han, Y.; Huang, F.; et al. 2023a. Qwen technical report. *arXiv preprint arXiv:2309.16609*.

Bai, J.; Bai, S.; Yang, S.; Wang, S.; Tan, S.; Wang, P.; Lin, J.; Zhou, C.; and Zhou, J. 2023b. Qwen-vl: A versatile vision-language model for understanding, localization, text reading, and beyond.

Bai, T.; Liang, H.; Wan, B.; Yang, L.; Li, B.; Wang, Y.; Cui, B.; He, C.; Yuan, B.; and Zhang, W. 2024. A Survey of Multimodal Large Language Model from A Data-centric Perspective. *arXiv preprint arXiv:2405.16640*.

Chen, L.; Li, J.; Dong, X.; Zhang, P.; He, C.; Wang, J.; Zhao, F.; and Lin, D. 2023. ShareGPT4V: Improving Large Multi-Modal Models with Better Captions. *CoRR*, abs/2311.12793.

Chen, Z.; Wu, J.; Wang, W.; Su, W.; Chen, G.; Xing, S.; Zhong, M.; Zhang, Q.; Zhu, X.; Lu, L.; et al. 2024. Internvl: Scaling up vision foundation models and aligning for generic visual-linguistic tasks. In *Proceedings of the IEEE/CVF Conference on Computer Vision and Pattern Recognition*, 24185–24198.

Cobbe, K.; Kosaraju, V.; Bavarian, M.; Chen, M.; Jun, H.; Kaiser, L.; Plappert, M.; Tworek, J.; Hilton, J.; Nakano, R.; et al. 2021. Training verifiers to solve math word problems. *arXiv preprint arXiv:2110.14168*.

He, Z.; Wu, X.; Zhou, P.; Xuan, R.; Liu, G.; Yang, X.; Zhu, Q.; and Huang, H. 2024. CMMU: A Benchmark for Chinese Multi-modal Multi-type Question Understanding and Reasoning. *arXiv preprint arXiv:2401.14011*.

Hendrycks, D.; Burns, C.; Kadavath, S.; Arora, A.; Basart, S.; Tang, E.; Song, D.; and Steinhardt, J. 2021. Measuring mathematical problem solving with the math dataset. *arXiv preprint arXiv:2103.03874*.

Jian, Y.; Gao, C.; and Vosoughi, S. 2023. Bootstrapping Vision-Language Learning with Decoupled Language Pre-training. In *Advances in Neural Information Processing Systems 36: Annual Conference on Neural Information Processing Systems 2023, NeurIPS 2023, New Orleans, LA, USA, December 10 - 16, 2023*.

Li, B.; Zhang, Y.; Chen, L.; Wang, J.; Yang, J.; and Liu, Z. 2023a. Otter: A Multi-Modal Model with In-Context Instruction Tuning. *CoRR*, abs/2305.03726.

Li, J.; Li, D.; Savarese, S.; and Hoi, S. 2023b. Blip-2: Bootstrapping language-image pre-training with frozen image encoders and large language models. In *International conference on machine learning*, 19730–19742. PMLR.

Li, J.; Li, D.; Savarese, S.; and Hoi, S. 2023c. Blip-2: Bootstrapping language-image pre-training with frozen image encoders and large language models. In *International conference on machine learning*, 19730–19742. PMLR.

Li, J.; Li, D.; Xiong, C.; and Hoi, S. C. H. 2022a. BLIP: Bootstrapping Language-Image Pre-training for Unified Vision-Language Understanding and Generation. In *International Conference on Machine Learning, ICML 2022, 17-23 July 2022, Baltimore, Maryland, USA*, volume 162, 12888–12900.

Li, L. H.; Zhang, P.; Zhang, H.; Yang, J.; Li, C.; Zhong, Y.; Wang, L.; Yuan, L.; Zhang, L.; Hwang, J.; Chang, K.; and Gao, J. 2022b. Grounded Language-Image Pre-training. In *IEEE/CVF Conference on Computer Vision and Pattern Recognition, CVPR 2022, New Orleans, LA, USA, June 18-24, 2022*, 10955–10965. IEEE.

Liu, H.; Li, C.; Li, Y.; and Lee, Y. J. 2023a. Improved baselines with visual instruction tuning. *arXiv preprint arXiv:2310.03744*.

Liu, H.; Li, C.; Wu, Q.; and Lee, Y. J. 2023b. Visual Instruction Tuning. In *Advances in Neural Information Processing Systems 36: Annual Conference on Neural Information Processing Systems 2023, NeurIPS 2023, New Orleans, LA, USA, December 10 - 16, 2023*.

Liu, H.; Li, C.; Wu, Q.; and Lee, Y. J. 2024a. Visual instruction tuning. *Advances in neural information processing systems*, 36.

Liu, H.; Zheng, Z.; Qiao, Y.; Duan, H.; Fei, Z.; Zhou, F.; Zhang, W.; Zhang, S.; Lin, D.; and Chen, K. 2024b. MathBench: Evaluating the Theory and Application Proficiency of LLMs with a Hierarchical Mathematics Benchmark. *arXiv preprint arXiv:2405.12209*.

Liu, S.; Zeng, Z.; Ren, T.; Li, F.; Zhang, H.; Yang, J.; Li, C.; Yang, J.; Su, H.; Zhu, J.; and Zhang, L. 2023c. Grounding DINO: Marrying DINO with Grounded Pre-Training for Open-Set Object Detection. *CoRR*, abs/2303.05499.

Lu, H.; Liu, W.; Zhang, B.; Wang, B.; Dong, K.; Liu, B.; Sun, J.; Ren, T.; Li, Z.; Sun, Y.; et al. 2024. Deepseek-vl: towards real-world vision-language understanding. *arXiv preprint arXiv:2403.05525*.

Lu, J.; Gan, R.; Zhang, D.; Wu, X.; Wu, Z.; Sun, R.; Zhang, J.; Zhang, P.; and Song, Y. 2023a. Lyrics: Boosting Fine-grained Language-Vision Alignment and Comprehension via Semantic-aware Visual Objects. *CoRR*, abs/2312.05278.

Lu, P.; Bansal, H.; Xia, T.; Liu, J.; Li, C.; Hajishirzi, H.; Cheng, H.; Chang, K.-W.; Galley, M.; and Gao, J.

2023b. Mathvista: Evaluating mathematical reasoning of foundation models in visual contexts. *arXiv preprint arXiv:2310.02255*.

OpenAI. 2023a. ChatGPT.

OpenAI, R. 2023b. Gpt-4 technical report. arxiv 2303.08774. *View in Article*, 2(5).

Radford, A.; Kim, J. W.; Hallacy, C.; Ramesh, A.; Goh, G.; Agarwal, S.; Sastry, G.; Askell, A.; Mishkin, P.; Clark, J.; et al. 2021. Learning transferable visual models from natural language supervision. In *International conference on machine learning*, 8748–8763. PMLR.

Reid, M.; Savinov, N.; Teplyashin, D.; Lepikhin, D.; Lilliacrap, T.; Alayrac, J.-b.; Soricut, R.; Lazaridou, A.; Firat, O.; Schriftwieser, J.; et al. 2024. Gemini 1.5: Unlocking multimodal understanding across millions of tokens of context. *arXiv preprint arXiv:2403.05530*.

Touvron, H.; Lavril, T.; Izacard, G.; Martinet, X.; Lachaux, M.-A.; Lacroix, T.; Rozière, B.; Goyal, N.; Hambro, E.; Azhar, F.; et al. 2023. Llama: Open and efficient foundation language models. *arXiv preprint arXiv:2302.13971*.

Wang, K.; Pan, J.; Shi, W.; Lu, Z.; Zhan, M.; and Li, H. 2024a. Measuring multimodal mathematical reasoning with math-vision dataset. *arXiv preprint arXiv:2402.14804*.

Wang, W.; Mrini, K.; Yang, L.; Kumar, S.; Tian, Y.; Yan, X.; and Wang, H. 2024b. Finetuned Multimodal Language Models Are High-Quality Image-Text Data Filters. *CoRR*, abs/2403.02677.

Wu, J.; Gan, W.; Chen, Z.; Wan, S.; and Yu, P. S. 2023. Multimodal large language models: A survey. *arXiv preprint arXiv:2311.13165*.

Xu, L.; Xue, H.; Zhu, L.; and Zhao, K. 2024a. SuperCLUE-Math6: Graded Multi-Step Math Reasoning Benchmark for LLMs in Chinese. *arXiv preprint arXiv:2401.11819*.

Xu, Y.; Liu, X.; Liu, X.; Hou, Z.; Li, Y.; Zhang, X.; Wang, Z.; Zeng, A.; Du, Z.; Zhao, W.; et al. 2024b. ChatGLM-Math: Improving Math Problem-Solving in Large Language Models with a Self-Critique Pipeline. *arXiv preprint arXiv:2404.02893*.

Yang, A.; Xiao, B.; Wang, B.; Zhang, B.; Bian, C.; Yin, C.; Lv, C.; Pan, D.; Wang, D.; Yan, D.; et al. 2023. Baichuan 2: Open large-scale language models. *arXiv preprint arXiv:2309.10305*.

Ying, H.; Zhang, S.; Li, L.; Zhou, Z.; Shao, Y.; Fei, Z.; Ma, Y.; Hong, J.; Liu, K.; Wang, Z.; et al. 2024. Internlm-math: Open math large language models toward verifiable reasoning. *arXiv preprint arXiv:2402.06332*.

Young, A.; Chen, B.; Li, C.; Huang, C.; Zhang, G.; Zhang, G.; Li, H.; Zhu, J.; Chen, J.; Chang, J.; et al. 2024. Yi: Open foundation models by 01. ai. *arXiv preprint arXiv:2403.04652*.

Yue, X.; Qu, X.; Zhang, G.; Fu, Y.; Huang, W.; Sun, H.; Su, Y.; and Chen, W. 2023. Mammoth: Building math generalist models through hybrid instruction tuning. *arXiv preprint arXiv:2309.05653*.

Zhang, H.; Zhang, P.; Hu, X.; Chen, Y.; Li, L. H.; Dai, X.; Wang, L.; Yuan, L.; Hwang, J.; and Gao, J. 2022. GLIPv2: Unifying Localization and Vision-Language Understanding. In *Advances in Neural Information Processing Systems 35: Annual Conference on Neural Information Processing Systems 2022, NeurIPS 2022, New Orleans, LA, USA, November 28 - December 9, 2022*.

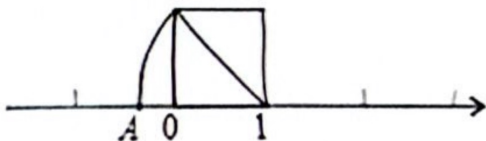
Zhang, R.; Jiang, D.; Zhang, Y.; Lin, H.; Guo, Z.; Qiu, P.; Zhou, A.; Lu, P.; Chang, K.-W.; Gao, P.; et al. 2024. Mathverse: Does your multi-modal lilm truly see the diagrams in visual math problems? *arXiv preprint arXiv:2403.14624*.

Zhao, W. X.; Zhou, K.; Li, J.; Tang, T.; Wang, X.; Hou, Y.; Min, Y.; Zhang, B.; Zhang, J.; Dong, Z.; et al. 2023. A survey of large language models. *arXiv preprint arXiv:2303.18223*.

A More Case Study

We present additional case studies. As shown in Figure 10 and Figure 11, the model struggles with complex reasoning tasks. This highlights the need to develop stronger reasoning models.

As shown in the figure, using a unit length segment on the number line as the side of a square, with the point representing the number 1 as the center of a circle, a semicircle is drawn with a radius equal to the side length of the square. The semicircle intersects the number line at point A. The number represented by point A is ____.



(a) Math Problem

Judge: The answer is incorrect.

Difficulty: Weak spatial ability and spatial position reasoning skills.

(c) Challenges

First, the problem describes a square with a side length equal to the unit length representing the number 1 on the number line. Let's denote the side length of this square as 1 unit. Next, the problem states that the point representing the number 1 is the center of a circle, and the radius of the arc is equal to the length of the diagonal of the square. We know that the length of the diagonal of a square is $\sqrt{2}$ times the side length, so in this case, the diagonal length is $\sqrt{2}$. Therefore, with 1 as the center and $\sqrt{2}$ as the radius, the length of this arc represents the distance on the number line. Simply put, the arc intersects the number line at point A, and the distance from point A to the origin (0) on the number line is $\sqrt{2}$.

So, the number represented by point A is 1 plus $\sqrt{2}$, which means point A represents the number $1 + \sqrt{2}$.

Final Answer: $1 + \sqrt{2}$

(b) GPT4 Response

Figure 10: Illustration of Case Study 2. The red sign marks the incorrect part of the answer.

When actually measuring the height of a mountain, you can measure the relative height between adjacent observable points among several observation points and then use these relative heights to calculate the mountain's height. The table below records some of the measurement data (e.g., A-C=90 shows A is 90 meters higher than C):

A-C	C-D	E-D	F-E	G-F	B-G
90	70	-60	50	-40	60

- 1) Based on the data of C-D and E-D, is observation point C higher or lower than observation point E? By how much?
- 2) How much higher is observation point A compared to observation point B?
- 3) How much higher is the highest observation point compared to the lowest observation point?

(a) Math Problem

(1) 130 meters;
(2) 150 meters;
(3) 220 meters

Challenges:

1. The reasoning chain is too long; involves six steps of reasoning.

2. Requires accurate memory ability.

Correct & Incorrect Answers:

Correct answers are marked as **green**.
Incorrect answers are marked as **red**.

(b) Correct Answer & Challenges

Based on the information provided in the image, let's first interpret the data in the table:

$$\begin{aligned} A - C &= 90 \text{ meters} \\ C - D &= 70 \text{ meters} \\ E - D &= -60 \text{ meters} \\ F - E &= 50 \text{ meters} \\ G - F &= -40 \text{ meters} \\ B - G &= 60 \text{ meters} \end{aligned}$$

Now, let's solve the questions step by step:

(1) First, let's compare the heights of observation points C and E. Since E - D is -60 meters, this means point D is 60 meters higher than point E. C - D is 70 meters, meaning point C is 70 meters higher than point D. Therefore, the height of point C relative to point E is the 70 meters that C is higher than D plus the 60 meters that D is higher than E, for a total of **130 meters**. Thus, observation point C is 130 meters higher than observation point E.

(2) We can calculate the height of point A relative to point B by combining the consecutive height differences:

$$\begin{aligned} A - C &= 90 \text{ meters} \\ C - B &= (C - D) + (D - E) + (E - F) + (F - G) + (G - B) \\ &= 70 + 60 + 50 + 40 + 60 \\ &= 280 \text{ meters} \end{aligned}$$

So, the height of point A relative to point B is $A - C + C - B = 90 + 280 = 370 \text{ meters}$.

(3) To find the highest and lowest observation points, we can observe the height differences relative to each other. From the data provided, the highest observation point is point A, and the lowest observation point is point E (as no point is lower than E). From the previous calculations, we already know that point A is 130 meters higher than point E. Since point A is 90 meters higher than point C, and point C is 130 meters higher than point E, we have:

The highest point A is 220 meters higher than the lowest point E:

$$A - E = A - C + C - E = 90 + 130 = 220 \text{ meters.}$$

This concludes the solution process. Here are the answers to each question:

- (1) The height difference by which observation point C is higher than observation point E: **130 meters**
- (2) The height of observation point A relative to observation point B: **370 meters**
- (3) The height difference between the highest and the lowest observation points: **220 meters**

(c) GPT4 Response

Figure 11: Illustration of Case Study 3. The red sign marks the incorrect part of the answer.

B Prompt for Scoring Answers

We summarize the prompt for scoring answers in Figure 12.

Task Description: Evaluate whether the student's answer to the given math problem is correct.

Input:

1. Problem Description: [Detailed description of the problem, including necessary mathematical formulas and conditions.] {question},
2. Reference Answer: [Detailed explanation of the correct answer, including the calculation process and result.] {answer},
3. Student's Answer: [The student's provided answer, including the calculation process and result.] {response},

Requirements:

- Carefully compare the student's answer with the reference answer.
- Analyze the correctness of the student's answer, including the calculation process and the final result.
- If the student's answer is incorrect, identify the error and briefly explain the reason for the mistake.
- Provide a concise evaluation conclusion, clearly stating whether the student's answer is correct.

Example:

Problem Description: Calculate the area of a triangle with a base of 6 cm and a height of 3 cm.

Reference Answer: (1) $\text{Area} = 0.5 * \text{base} * \text{height} = 0.5 * 6 \text{ cm} * 3 \text{ cm} = 9 \text{ cm}^2$.

Student's Answer: (1) $\text{Area} = 6 \text{ cm} * 3 \text{ cm} = 18 \text{ cm}^2$.

Evaluation:

(1) False, explanation as follows:

- The student's calculation process ignored the 1/2 coefficient in the area formula.
- The result is incorrect; the correct calculation should yield 9 cm^2 , not 18 cm^2 .
- Conclusion: The student's answer is incorrect.

Based on the above task description and requirements, compare the reference answer and the student's answer in order. Carefully consider whether they are consistent.

2. If the student's answer is correct, output True; otherwise, output False and provide an evaluation conclusion.

You need to output:

Only the True or False for each question, example: Judgement result: (1) True, (2) False, (3) True
Explanation as follows: (1)... (2)... (3)...

Figure 12: Prompt used for scoring answers.

C Visualization of MathScape

C.1 Visualization of Performance of Different Models.

We include additional math samples in MathScape, as illustrated in Figure 13.

There are 24 investors who want to invest in a certain place, and their ages are numbered from small to large as 1-24 as shown in the figure. Then, 6 investors are selected by systematic sampling method and invited to visit the site. Among them, the number of investors who are not more than 55 years old is _____.

A. 1 B. 2 C. 3 D. 4

3	9
4	0 1 1 2 5
5	1 3 6 6 7 7 8 8 8 9
6	0 0 1 2 3 3 4 5

The height of a mountain can be measured by measuring the relative heights of each of the two adjacent visual observation points in several observation points, and then using these relative heights to calculate the height of the mountain. The table below is a partial record of one measurement.

(1) According to C-D and E-D data, is the comparison observation point C higher or lower than the relative observation point E?

A-C	C-D	E-D	F-E	G-F	B-G
90m	70m	-60m	50m	-40m	60m

Given that $AM \parallel BN$, $\angle A = 60^\circ$, point P is a moving point on the ray AM (not coincident with A), BC and BD bisects $\angle ABP$ and $\angle PBN$ respectively, and the intersection ray AM is at C and D. (To have the reasoning process, do not need to write the reason for each step)

Try to prove: $\angle APB = 2\angle ADB$

Point $M(x, y)$ is an internal dynamic point within the shadow area, which of the option is true ?

A. $\sin(x+y) > 0$ C. $\cos(x+y) > 0$
 B. $\sin(x+y) < 0$ D. $\cos(x+y) < 0$

Figure 1 shows a rectangle $2m$ in length and $2n$ in width, which is divided into four small rectangles with scissors along the dotted line in the figure, and then assembled into a square according to Figure 2.

You believe that the length of the side of the shaded square in Figure 2 is equal to _____.

Figure 1: A rectangle with length $2m$ and width $2n$, divided into four smaller rectangles by dashed lines.

Figure 2: A square formed by assembling the four smaller rectangles from Figure 1. A small shaded square is located in the center of the square.

Calculate the surface area and volume of the following cube.

Figure 13: Math problem samples in MathScape.